Global Environmental Science
www.sciltp.com/journals/ges

Supplementary Materials

Hierarchical Sandwich-Type Hetero-Wetting Nanofibrous Membrane toward Nano-Scaled Oil/Water Emulsion Separation

Linlin Yan [1,2], Mengmeng Zhang [1], Chen Chen [1], Mi Zhou [1], Kai Wang [1,2], Yuhua Gao [3], Pengcheng Liu [2], Dalong Li [1] and Xiquan Cheng [1,2,*]

[1] State Key Laboratory of Urban-rural Water Resource and Environment, School of Marine Science and Technology, Harbin Institute of Technology, Weihai 264209, China
[2] Weihai Key Laboratory of Water Treatment and Membrane Technology, Shandong Sino-European Membrane Technology Research Institute Co., Ltd., Weihai 264209, China
[3] Institute of Energy Resources, Hebei Academy of Sciences, Shijiazhuang 050081, China
* Correspondence: chengxiquan@hit.edu.cn

How To Cite: Yan, L.; Zhang, M.; Chen, C.; et al. Hierarchical Sandwich-Type Hetero-Wetting Nanofibrous Membrane toward Nano-Scaled Oil/Water Emulsion Separation. *Glob. Environ. Sci.* **2026**, *2*(1), 53–66. https://doi.org/10.53941/ges.2026.100005

1. Experimental Section

1.1. The Water Uptake Capacity of the Membranes

The membranes were initially weighed in their dry state prior to submersion in DI water for 24 h at normal temperature. Then, surface-adhered water was carefully removed using lint-free blotting paper to determine the wet mass of the membranes. The water uptake of the membranes was subsequently calculated using the following equation.

$$W_{up} = \frac{W_{wet} - W_{dry}}{A} \quad \text{(S1)}$$

where Wup (g·m^{-2}) represents the water uptake, W_{wet} (g) and W_{dry} (g) means the membrane weight in the wet and dry state, respectively, A is the area of the membrane.

1.2. The Porosity of the Membranes

The porosity of the membranes was quantified through gravimetric measurements of dry membranes and those saturated with ethylene glycol. The density of the polymer was determined by testing with an electronic density balance (FA2104J). The porosity of the membranes was acquired by the following equation.

$$\varepsilon(\%) = \frac{\frac{m_1 - m_0}{\rho_1}}{\frac{m_1 - m_0}{\rho_1} + \frac{m_0}{\rho_0}} \times 100\% \quad \text{(S2)}$$

where m_1 and m_0 are the masses of the wetted and dried membranes, respectively, while ρ_1 and ρ_0 are the densities of ethylene glycol and polymer, respectively.

1.3. The Apparent Surface Energy of the Membranes

The apparent surface energy of the fabricated membranes was determined using WCAs and diiodomethane contact angles based on the following equations.

$$\gamma_l(1 + cos\theta) = 2\left(\gamma_l^p \gamma_m^p\right)^{1/2} + 2\left(\gamma_l^d \gamma_m^d\right)^{1/2} \quad \text{(S3)}$$

$$\gamma_m = \gamma_m^d + \gamma_m^p \quad \text{(S4)}$$

where γ represents apparent surface energy, with subscripts l and m indicating the test liquid and membrane, respectively. Superscripts d and p denote dispersive and polar components, respectively. θ refers to the contact angles.

1.4. The Content of Different Forms of Water in Membranes

The thermal behavior and hydration states of the nanofiber films were investigated using a differential scanning calorimeter (Bruker DSC 3100SA, Germany). Measurements were conducted under nitrogen atmosphere with a heating rate of 5 °C/min across a temperature range of −70 °C to 100 °C. Three distinct hydration states were identified through thermal analysis: free water, frozen bound water and non-frozen bound water. The non-frozen water, exhibiting strong hydrogen bonding with hydrophilic groups on the membrane surface, critically influences the material's hydration capacity. Quantification of water states was performed using the following equations:

$$W_s(\%) = \frac{m_1 - m_0}{m_1} \times 100\% \quad \text{(S5)}$$

$$W_{fs}(\%) = \frac{\Delta H_s}{\Delta H_w} \times 100\% \quad \text{(S6)}$$

$$W_{nfs}(\%) = W_s - W_{fs} \quad \text{(S7)}$$

where m_0 and m_1 represent the dry mass and the wet mass of the membranes after soaking in water for 24 h, respectively. W_s (%) is the relative water absorption of the membranes, W_{fs} (%) and W_{nfs} (%) represent the freezable water fraction and non-freezable water fraction in the membranes, respectively. ΔH_s denotes the integrated melting enthalpy derived from DSC thermograms, while $\Delta H_w = 333.5$ (J·g^{-1}), corresponds to the theoretical enthalpy of pure ice fusion.

2. Supplementary Figures

As the PDMS concentration increased from 2% to 8%, the permeance increased from 15,990 L·m^{-2}·h^{-1}·bar^{-1} to 22,308 L·m^{-2}·h^{-1}·bar^{-1} and the separation efficiency increased from 99.89% to 99.97%. However, further increases in PDMS concentration led to a decrease in the oil-water separation permeance and separation efficiency. Therefore, PDMS concentration of 8% was determined to be the optimal concentration for the intermediate layer.

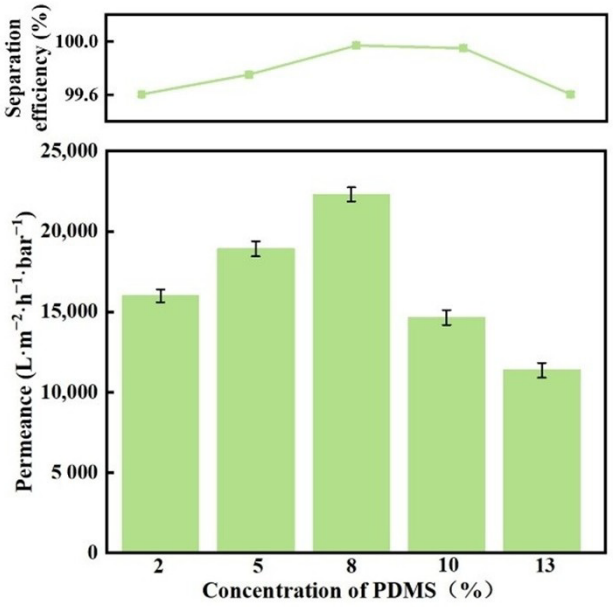

Figure S1. Emulsion permeance and separation efficiency of PAN-PP/PDMS/PAN-PP membrane.

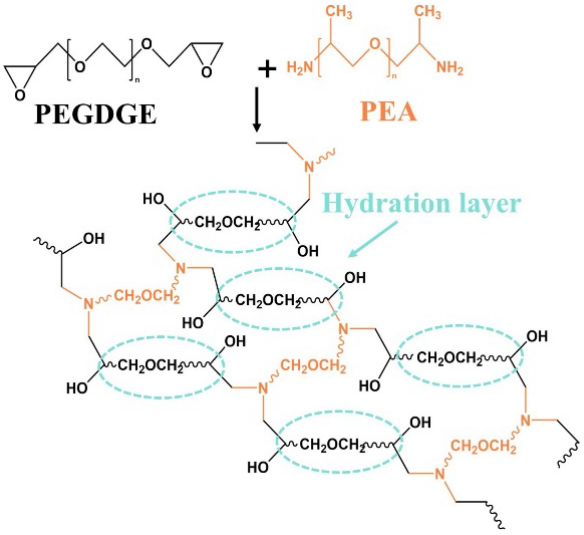

Figure S2. Speculated mechanisms of ring-opening-reaction induced PEA/PEGDGE hybridization to realize *in-situ* hydrophilization in PAN-based membranes.

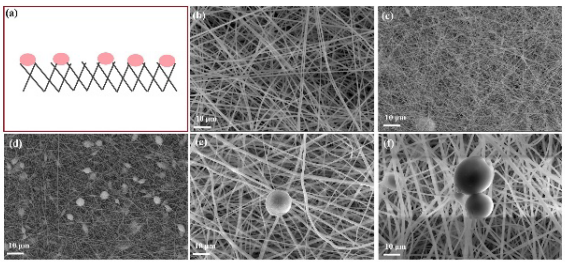

Figure S3. (**a**) Schematic illustration of the PDMS/PAN-PP membrane. SEM images of the PDMS/PAN-PP membrane fabricated at different PDMS concentration conditions of (**b**) 2%; (**c**) 5%, (**d**) 8%; (**e**) 10%; (**f**) 13%.

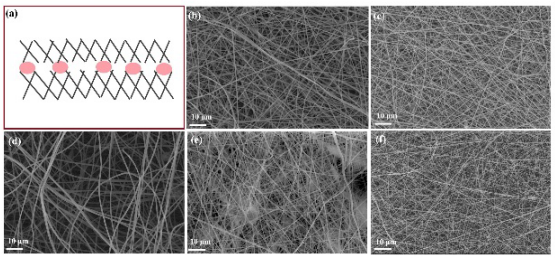

Figure S4. (**a**) Schematic illustration of the PAN-PP/PDMS/PAN-PP membrane. SEM images of the PAN-PP/PDMS/PAN-PP membrane fabricated at different PDMS concentration conditions of (**b**) 2%; (**c**) 5%; (**d**) 8%; (**e**) 10%; (**f**) 13%.

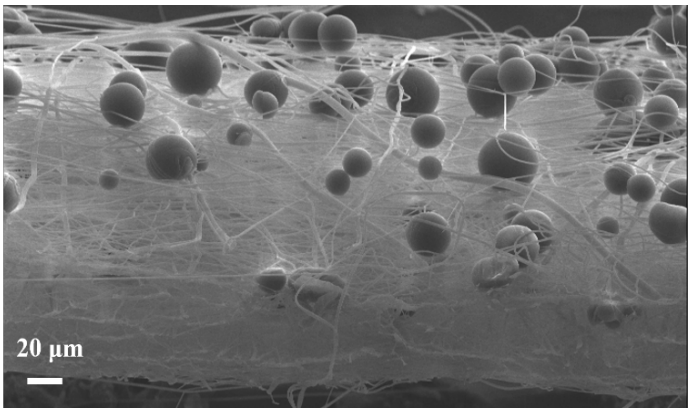

Figure S5. Cross-sectional SEM image of the PDMS/PAN-PP membrane.

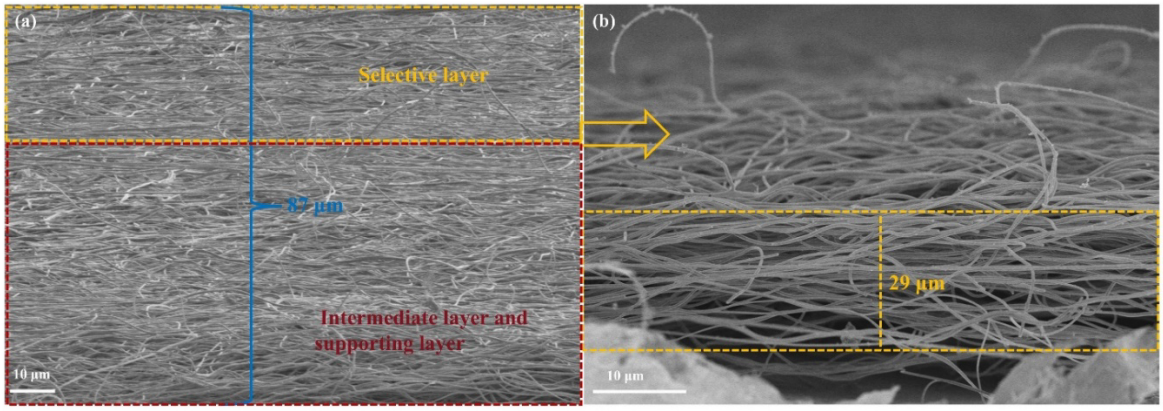

Figure S6. (**a**) Cross-sectional SEM image of the PAN-PP/PDMS/PAN-PP membrane; (**b**) SEM image of the selective layer on the PAN-PP fiber.

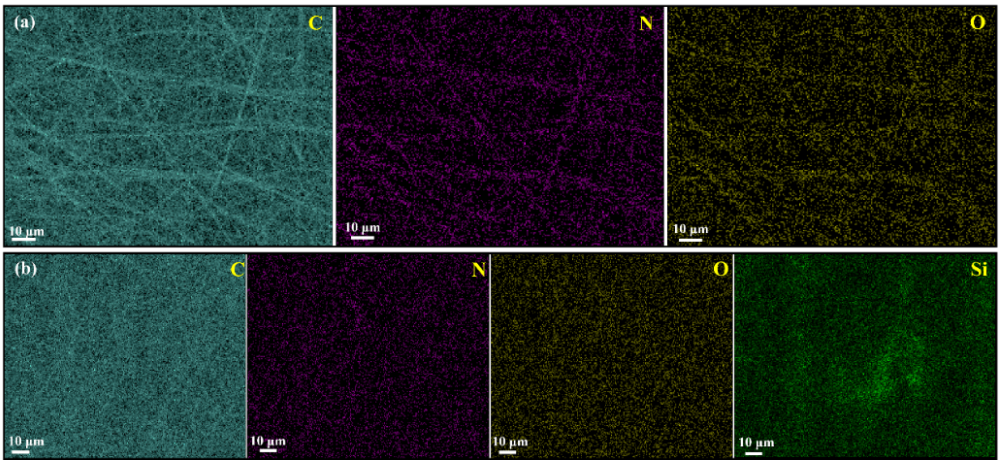

Figure S7. Elemental mapping images of (**a**) PAN-PP and (**b**) PAN-PP/PDMS/PAN-PP membranes.

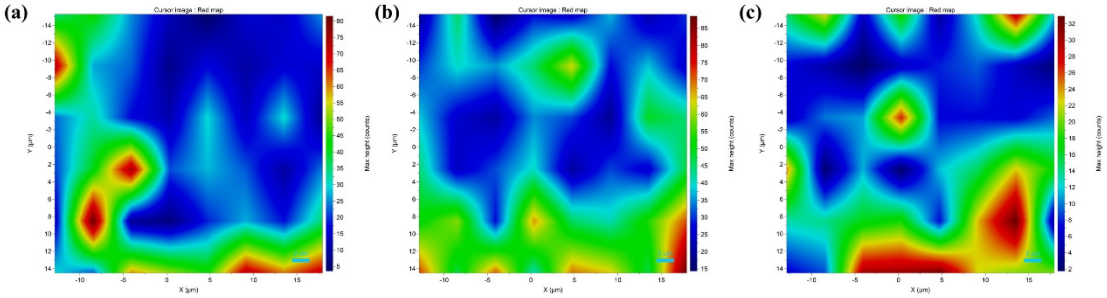

Figure S8. Two-dimensional Raman surface scanning of (**a**) PDMS/PAN-PP and (**b**,**c**) PAN-PP/PDMS/PAN-PP membranes.

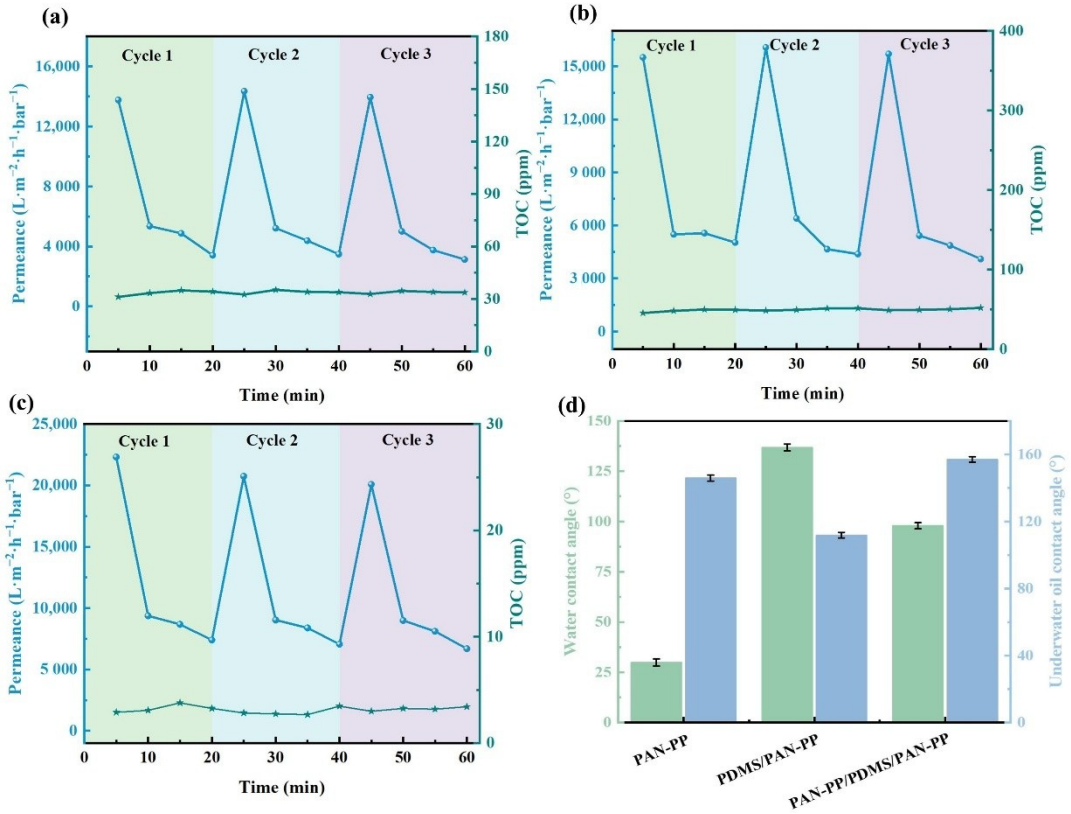

Figure S9. Long separation cycle performance of (**a**) PAN-PP; (**b**) PDMS/PAN-PP and (**c**) PAN-PP/PDMS/PAN-PP membranes; (**d**) The WCA and UOCA of the PAN-PP/PDMS/PAN-PP membrane before and after 20 separation cycles.

Table S1. The content of different forms of water in as-prepared membranes.

Membrane	W_s (%)	W_{fs} (%)	W_{nfs} (%)
PAN-PP	86.02	7.40	78.62
PDMS/PAN-PP	78.69	1.89	76.80
PAN-PP/PDMS/PAN-PP	95.85	13.00	82.85

 https://doi.org/10.53941/ges.2026.100005